Rationally designed hydrophllic ZIF-rGO hybrids for bifunctional detection of trace Pb^{2+} and Cd^{2+} in river water

Hongyan Xu[1]*, Chengkai Xia[2]*, Junrui Qu[2], Xiangpeng Zeng[2], Wantong Zhu[2], Ying Hou[2], Siyan Wang[2], Miao Yu[1]

1 Laoshan Laboratory, Qingdao 266237, China

2 School of Materials Science and Engineering, MOE jointly Collaborative Innovation Center for High-performance Al/Mg based Materials, Shanxi Key Laboratory of Intelligent Casting and Advanced Forming for New Materials, North University of China, Taiyuan 030051, PR China

*Corresponding author

E-mail address: xuhongyan@nuc.edu.cn *(Prof. Hongyan Xu)*

ckxia@nuc.edu.cn *(Prof. Chengkai Xia)*

Preparation of LAA-X-rGO

LAA-X-rGO was successfully prepared using a simple chemical reduction process using L-ascorbic acid, as shown in **Figure 1**. First, graphite oxides (GO) were acquired using the modified Hummers method. Then 100 mg GO were added to 100 mL deionized water and ultrasonically dispersed for 30 min to get the GO suspension, followed with the decanting of 100 mL L-AA solution. The above mixture was heated at 80 ℃ for 2h. After cooling down to room temperature, the mixture was centrifugal washed using ethanol for several times and dried at 80 ℃ in oven to obtain the reduced graphite oxides (rGO). In order to investigate the effect of hydrophilic/hydrophobic properties on the electrochemical properties of rGO, the quality ratios of L-AA to GO were set as 0.1, 0.3, 0.5, 0.7 and 0.9, the corresponding rGO products were labeled as LAA-X-rGO, X= 0.1, 0.3, 0.5, 0.7 and 0.9.

Preparation of Half-carbonized ZIF

2.1 g of 2-methylimidazole was dissolved in deionized water, and 5 mmol of NaOH was dissolved in deionized water; the two solutions were then mixed and designated as solution A. Subsequently, 0.24 mmol of cobalt nitrate hexahydrate and 0.36 mmol of zinc nitrate hexahydrate were separately dissolved in deionized water and designated as solution B. Solutions A and B were mixed and stirred for 4 h. The resulting mixture was centrifuged and washed three times with ethanol, followed by vacuum drying at 60 °C, yielding the product denoted as ZIF. The as-prepared ZIF was placed in a tube furnace under an air atmosphere and then annealed at 350 °C for 2

hours, and then finally achieved half-carbonized ZIF.

Preparation of electrodes

Firstly, 1 mg sensitive materials were added to 4 mL ethanol and dispersed ultrasonically for 30 min to obtain 0.25 mg/mL sensitive materials dispersion solution. Then, 5 μL of the above obtained sensitive materials dispersion solution waas drop-casted using a pipette gun on the polished GCE (Φ=3 mm) and dried in air. Finally, 5 μL 0.5 wt% Nafion solution was cover on this electrode to obtain the modified GCE.

Measurements of electrochemical surface area

According to the scan-rate dependent CV measurements, the electrochemical effective areas of different working electrodes can be calculated by the following Randles-Sevcik equation [47].

$$I_p = (2.69 \times 10^5)\, n^{3/2}\, AcD^{1/2}v^{1/2}$$

where, I_p is the peak current value of the cyclic voltammetry curve at different scan rates (μA),

A is the electrochemical effective area (cm^2),

v is the scanning rate in the cyclic voltammetry test ($V \cdot s^{-1}$),

D is the diffusion coefficient of potassium ferricyanate solution (7.6×10^{-6} $cm^2 \cdot s^{-1}$),

n is the electron transfer number,

c is the concentration of potassium ferricyanate solution ($mol \cdot mL^{-1}$).

The CV curves with series of scan-rate and the corresponding fitting curves are shown in **Figure S5**. **Table S2** lists the electrochemical surface area (ECSA) values for different working electrodes.

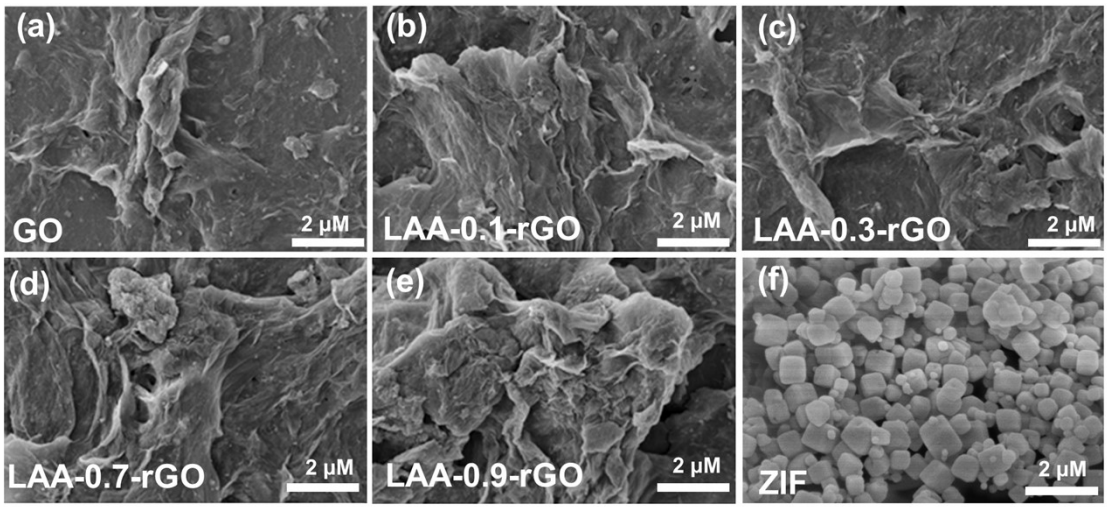

Figure S1 SEM image of GO (a), L-AA-0.1-rGO (b), L-AA-0.3-rGO (c), L-AA-0.7-rGO (d), and L-AA-0.9-rGO (e) ZIF.

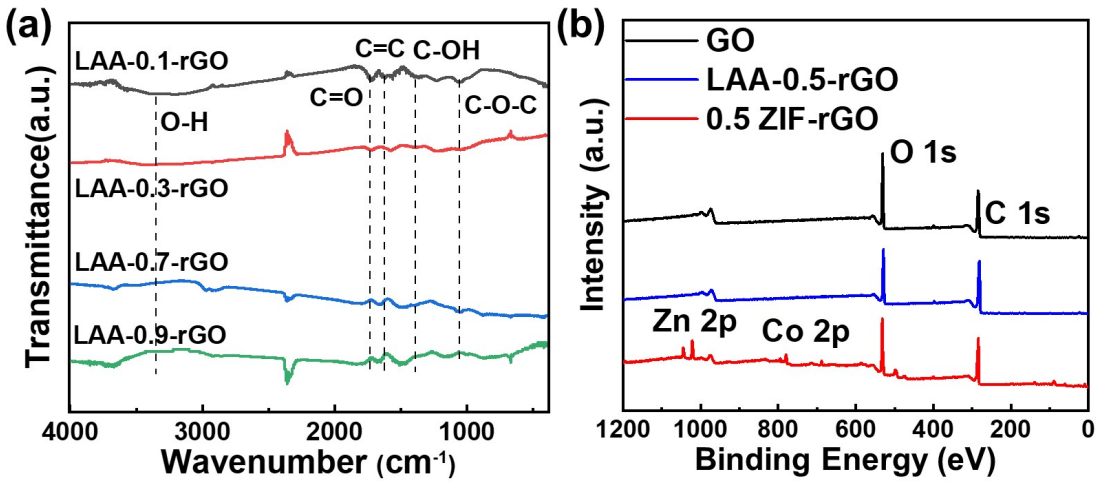

Figure S2 (a) FT-IR spectrum of the as-synthesized LAA-X-rGO samples. (b) XPS spectrum of the survey spectrum

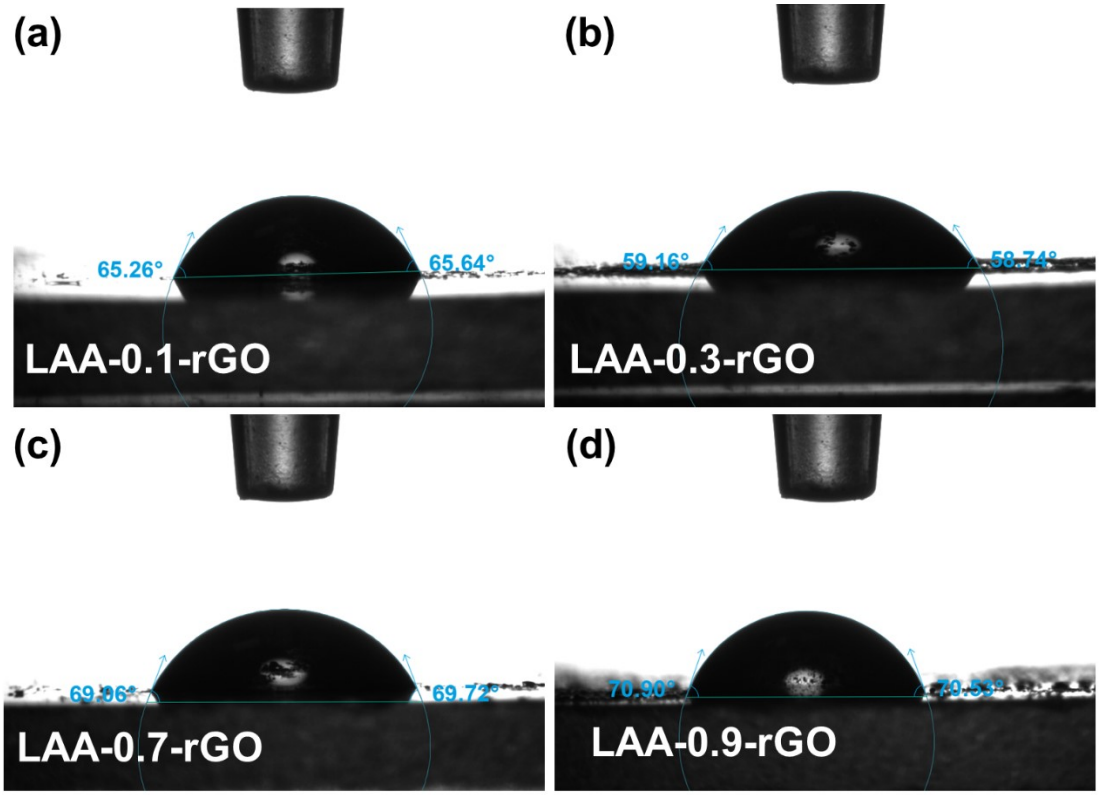

Figure S3 Contact angles of LAA-X-rGO

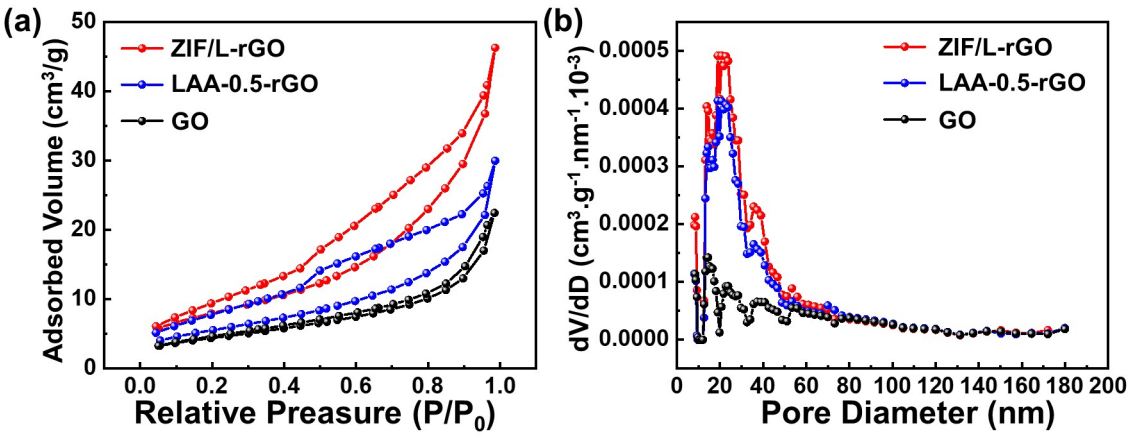

Figure S4 (a) BET nitrogen adsorption-desorption isotherm and (b) BJH pore size distribution curve of of GO, LAA-0.5-rGO, and ZIF/L-rGO.

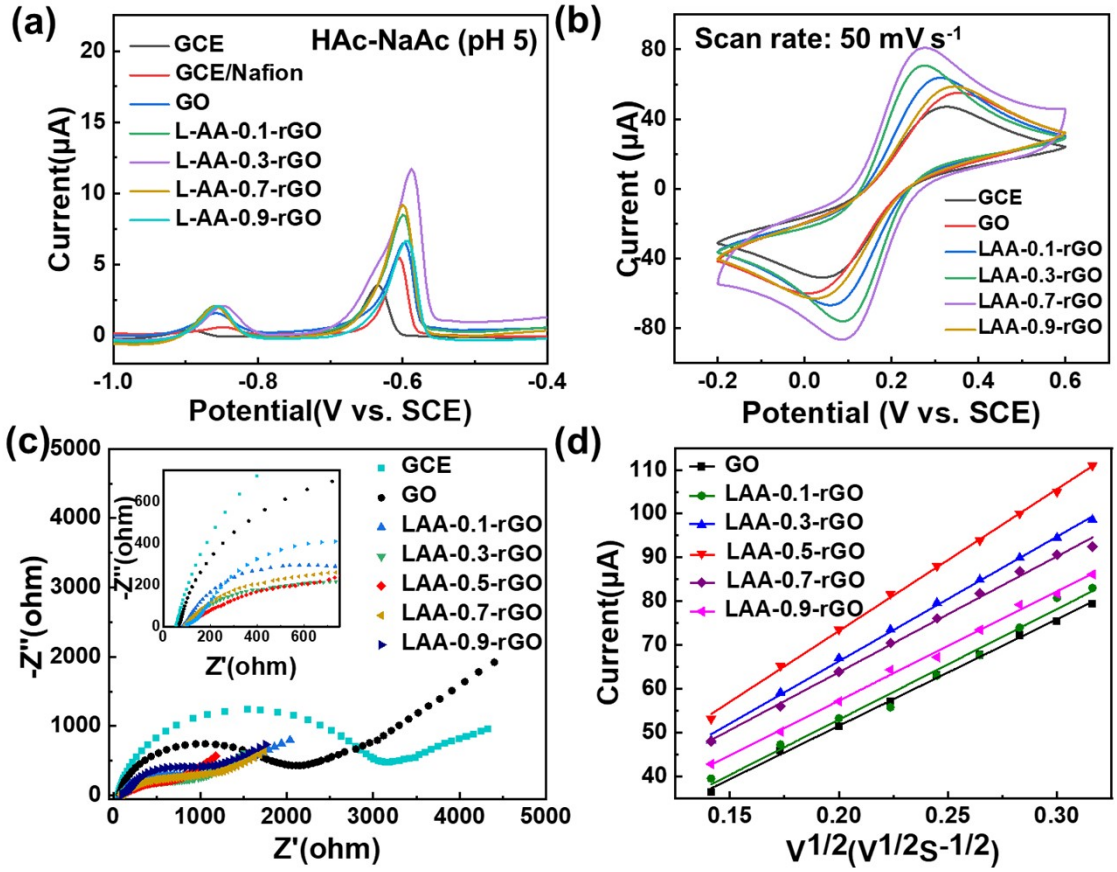

Figure S5 (a) DPASV curves tested with GCE, GO, and LAA-X-rGO decorated electrodes in HAc-NaAc solution (pH=5) with 2μM Pb^{2+} and Cd^{2+}. (b) CV curves (c) and Nyquist plots of GCE, GO, and LAA-X-rGO decorated electrodes in 0.1 mol/L KCl solution with 5.0 mmol/L $K_3[Fe(CN)_6]$. (d) The capacitance current of GO, LAA-X-rGO at scan rates of 10–90 mV s^{-1}

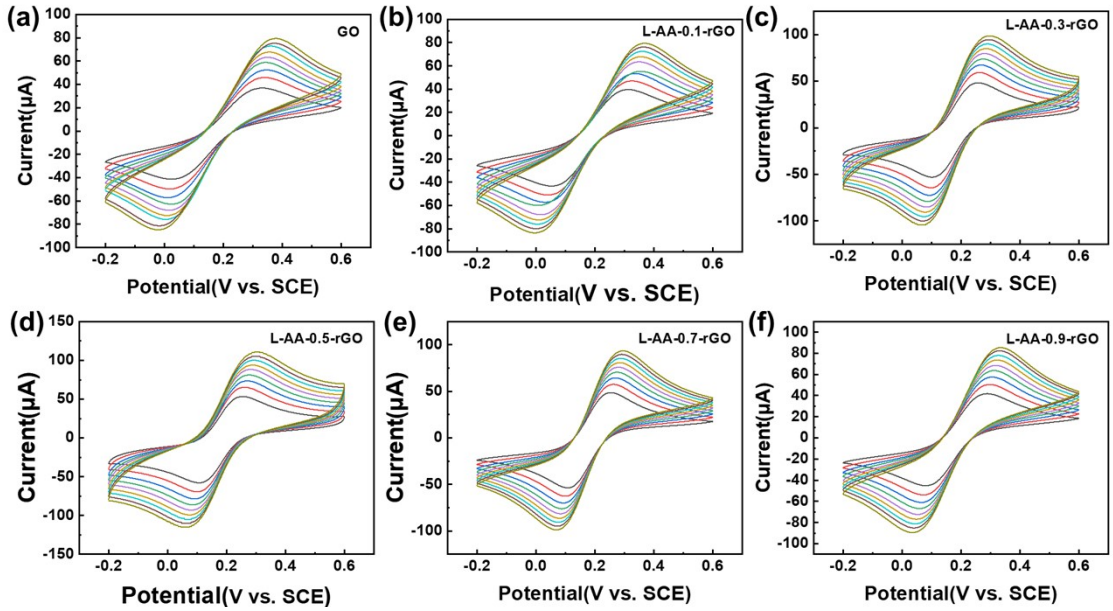

Figure S6 CV curves with series of scan-rate and the corresponding fitting curves for LAA-X-rGO

Table S1 The atomic percentage of GO, LAA-0.5-rGO, and ZIF/L-rGO

	O 1s	C 1s	Co 2p	Zn 2p
LAA-0.5-rGO	13.78%	86.21%	0	0
GO	31.22%	68.77%	0	0
ZIF/L-rGO	18.27%	76.79%	1.95	2.98

Table S2 Resistance values of the samples in the equivalent circuit

	R_s (Ω)	R_{ct} (Ω)
ZIF/L-rGO	9.78	346.6
LAA-0.5-rGO	8.49	1128
GO	6.11	2125

Table S3 The electrochemical effective areas of different working electrodes

Working electrode	Electrochemical surface area (cm^{-2})
GO	$5.42x10^{-2}$
LAA-0.5-rGO	$5.62x10^{-2}$
ZIF/L-rGO	$6.71x10^{-2}$

Table S4 Analytical results of ZIF/L-rGO decorated electrode in river water with different contents of Pb^{2+} and Cd^{2+}

Analys	Original	Added (μM)	Detected by DPASV (μM)	Recovery (%)
Pb^{2+}	ND	3	2.881	96.02
	ND	1	0.978	97.79
Cd^{2+}	ND	3	2.935	97.84
	ND	1	1.007	100.71

Table S5 Comparison of different electrodes in the electrochemical detection of heavy metal ions

Working electrode	Technique	Sensitivity (μA μM^{-1})		LOD (nM)		Ref.
		Pb^{2+}	Cd^{2+}	Pb^{2+}	Cd^{2+}	
ALA-pNE-rGO/GCE	DPASV	1.222	0.539	5.94	12.45	[1]
Cu-L@GCE	DPASV	3.89	1.28	2.12	13.63	[2]
C/$Bi_4O_5Br_2$/GCE	DPASV	1.485	3.66	4.78	2.89	[3]
Ag@ZIF-1000/GCE	DPASV	8.91	4.76	7.28	14.63	[4]
PtND-CA-SnNP/ITO	DPASV	5.18	12.43	9.66	13.16	[5]
CCO@CNCs-2/GCE	DPASV	13.95	9.816	1.54	1.13	[6]
ZIF/L-rGO /GCE	DPASV	6.92	2.41	8.67	24.01	This work

Reference

1. M. Patel, P. Prabhakar, P. Kumar, J. P. Chaurasia, A. K. Shrivastava, N. Dwivedi and C. Dhand, Polynorepinephrine enhanced synergism boost the detection of Cd2+ and Pb2+ ions with graphene oxide-based electrochemical sensors, *Microchemical Journal*, 2025, **216**, 114739.
2. T.-T. Guo, B.-L. Hua, Z.-Y. Guo, M.-Q. Zhang, J.-R. Wang, Y.-Y. An, X.-N. Li and J.-Z. Yan, A copper(ii)-based metal–organic framework: electrochemical sensing of Cd(ii) and Pb(ii) and adsorption of organic dyes, *Dalton Transactions*, 2025, **54**, 1393-1401.
3. Y. Qiao, Q. Zhang, Y. Wang, J. Yu, Z. Chen, J. Yang, J. Hu and H. Hou, One-step pyrolysis synthesis of C/Bi4O5Br2 nanocomposites for simultaneous electrochemical detection of Cd2+, Pb2+, and Zn2+ with high selectivity and sensitivity, *Sensors and Actuators B: Chemical*, 2025, **427**, 137169.
4. S. Wang, Y. Zhao, C. Xia, W. Zhu, Y. Hou, X. Zeng and H. Xu, Calcination-induced enhancement of Cd2+ and Pb2+ electrochemical detection capabilities of nano-ag-supported CoZn bi-metal ZIFs, *Environmental Science: Nano*, 2024, **11**, 2061-2072.
5. N. H. Ramli, N. Mohamad Nor, Z. Lockman and K. Abdul Razak, Fabrication of tin nanoparticles with functionalized platinum nanodendrites on ITO electrode for simultaneous detection of Cd2+, Pb2+, and Cu2+ ions, *Results in Chemistry*, 2025, **13**, 102013.
6. L. Xu, Y. Ran, M. Li, P. Huang, A. Farid, H. Huang and Y. Zhao, Constructing

cobalt-based heterogeneous composites in porous charge transfer network enabled by the spiral structure for efficient detection of Cd2+ and Pb2+, *Chemical Engineering Journal*, 2025, **514**, 162776.